

# 2D numerical simulation of meander morphology

*Mohd. Sarfaraz Banda*<sup>1</sup>, *Stephan Niewerth*<sup>1</sup>, and *Jochen Aberle*<sup>1,\*</sup>

<sup>1</sup>Leichtweiß-Institute for Hydraulic Engineering and Water Resources (LWI), TU Braunschweig, Braunschweig, Germany

**Abstract.** This paper describes the application of the two-dimensional (2D) modelling approach implemented in the open-source code Delft3D for the simulation of morphological development of a natural meandering river. A specific reach of the Dhaleshwari River (Bangladesh) for which field data has been available served as case study. The bed morphology and meander planform adjustment in the study area were simulated over a 10-year period considering a time-varying discharge scenario. The results showed that the 2D model was able to reproduce morphological characteristics such as scour depth, bank erosion and pool-riffle morphology, even though the model showed some deficiencies to reproduce bankfull channel width and transverse bed slopes. Regarding the planimetric evolution, the planform parameters (i.e., meander belt width, meander wavelength and radius of curvature) confirmed that the model results are realistic and are in agreement with results reported in the literature.

## 1. Introduction

The need for the prediction of the planform of natural meandering rivers arises from the fact that the migration of their channels can threaten the infrastructure as well as the safety and effectivity of hydraulic structures. This means that the dynamic evolution of meandering rivers can impose significant problems for water resources management. A promising tool to investigate the morphological development of natural meandering rivers is the use of numerical models. One-dimensional (1D) models can be used to capture the shifting of the channel centreline (e.g., [1-2]) but bed topography changes cannot be reproduced accurately with such models due to lack of information with regard to the transverse flow field, especially in the meander bends. Multi-dimensional (2D or 3D) models have the potential to overcome this limitation as they offer the possibility to reproduce the flow patterns in meander bends as well as the associated bed topography

---

\* Corresponding author: [jochen.aberle@tu-braunschweig.de](mailto:jochen.aberle@tu-braunschweig.de)

[e.g., 3-4]. Depth-averaged 2D models are often adopted in practice because the computational time is at least one order of magnitude shorter than for a 3D model [4-5]. Most of the existing numerical modelling studies on meandering rivers have been used to reproduce results from laboratory investigations (e.g., [6]) or have focused on hypothetical rivers (e.g., [7]). However, their application to simulate the morphological development of natural meandering rivers is scarce. This can be attributed to the fact that only few field data sets exist which cover typical morphological time-scales of years to decades, i.e. field data sets allowing for model validation.

Using field data from the meandering Dhaleshwari River in Bangladesh, the objective of the present study is to explore the capability of the open-source code Delft3D to simulate the adaption of both planform dynamics and bed topography of natural meandering rivers. Section 2 describes the study area and the available data and Section 3 describes the numerical model. Results are presented and discussed in Section 4.

## 2. Study area and available data

### 2.1. Location of the study area

The study area is located in the upper reach of the Dhaleshwari River which is one of the main distributaries of the Jamuna River in Bangladesh. It starts approx. 10 km downstream of Elashin gauging station (68A) and ends ca. 33.3 km upstream of Taraghat gauging station (137A) (see Fig. 1). In the study area, the river can be described as a well-developed meandering sand-bed channel (bankfull width in 2013 approx. 250 - 270 m) which is characterized by four consecutive meander bends. Historical and recent changes of the river in this reach have been documented (e.g., [8]) and data were available to set up, calibrate, and validate a numerical model (see [4] for details).

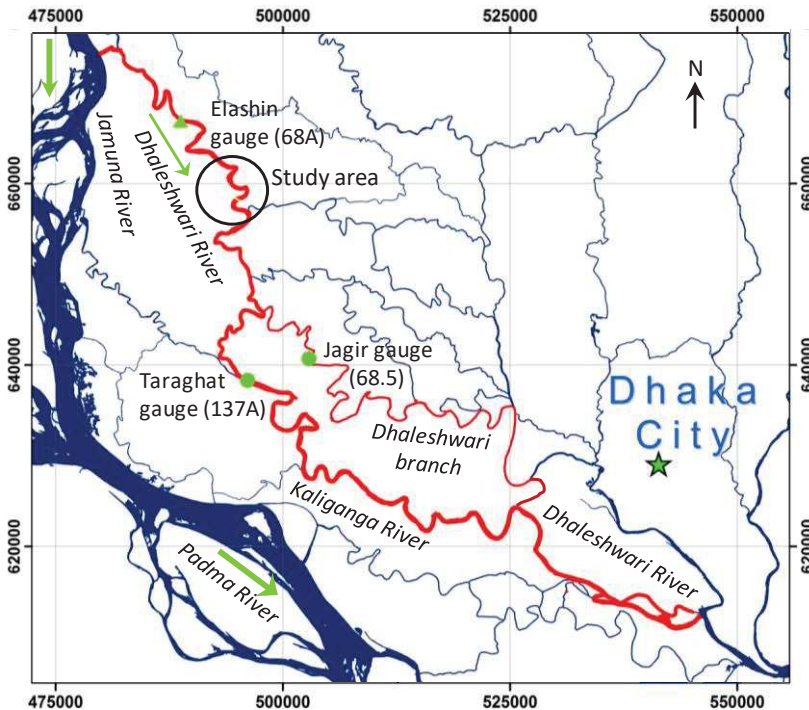
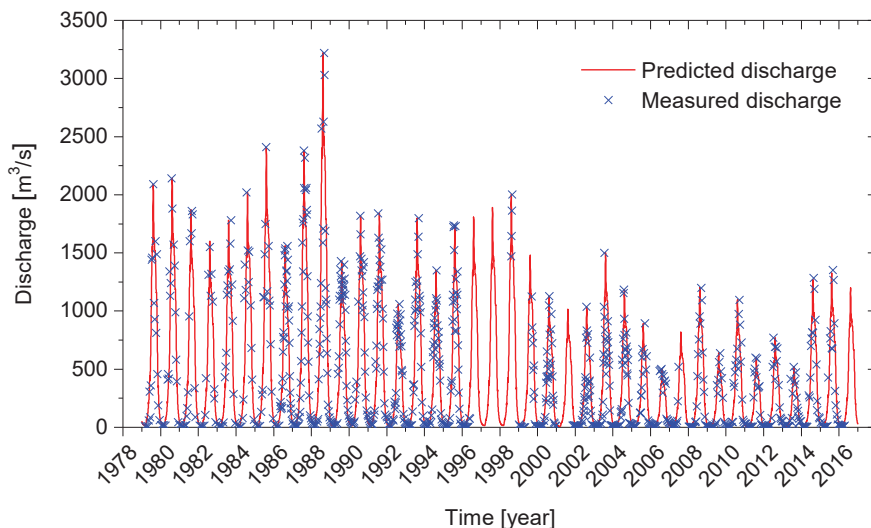


Fig. 1. Location of the study area.

## 2.2. Hydrological data

Hydrological data were available from the Bangladesh Water Development Board (BWDB) gauging stations (see Fig. 1 for their locations). Elashin gauging station (68A) records only water levels while the Taraghat (137A) gauging station at the Kaliganga River and the Jagir (68.5) gauging station on the Dhaleshwari branch record discharges and water levels. Note that the Dhaleshwari River flows into the Kaliganga River and that the Dhaleshwari branch is merely a flood spill channel of the Dhaleshwari River [8]. Therefore, for simplicity, the discharge of the Dhaleshwari River in the study area can be assumed to be the same as the discharge in the Kaliganga River.

The available data on river discharge had a few gaps or periods of missing data. To interpolate streamflow data at daily intervals, a Matlab script (Hydro Fit Curve) was developed and applied to 37 years of streamflow data. The script is based on a statistical mean standard curve, which is the average of the yearly discharge curves, normalized with the maximum discharge of that year. In case of missing data, the maximum discharges were interpolated by fitting a cubic spline function over all available maximum discharges. The record of synthetic daily flows is compared with the observed data in Fig. 2. The Nash-Sutcliffe efficiency index [9] of 0.85 showed the good agreement of the fitted with the measured data. Note also that, for a discharge of  $615 \text{ m}^3 \text{ s}^{-1}$ , the water surface elevations within the study area were available from a field campaign.



**Fig. 2.** Continuous time-series of daily discharge in the period 1979 - 2016.

## 2.3. Morphological data

The river bed and the banks in the study area consist of fine sand with a median diameter ( $D_{50}$ ) of 0.1 mm [4]. A sediment rating curve for the Dhaleshwari River was developed based on data measured at Taraghat gauging station (137A) in the period 1971 - 1996. Two monitoring cross-sections (one at the upstream end and the other at 1.64 km upstream from the downstream end) were located within the study area and measurements of bed level changes were provided by BWDB. Cross-sections from the year 2003 were used to construct the digital elevation model (DEM) (see [4] for more details).

### 3. The numerical model

This section describes briefly the open source code Delft3D (<https://oss.deltares.nl/web/delft3d>) and the way in which it has been used in this study. The standard hydrostatic version of Delft3D-Flow was used to model the morphological changes taking place over 10 years in a 8.2 km long section of the study area. The computational mesh was constructed in a curvilinear coordinate system which is the most appropriate coordinate system to account for the meandering planform. The digital elevation model (DEM) from the year 2003 was used as the initial bathymetry for the simulations.

#### 3.1. Hydrodynamics

For the present study, the 2D modelling approach implemented in Delft3D was used. The flow was modelled based on the conservation of momentum (Eq. 1 and 2) and conservation of mass (Eq. 3), assuming hydrostatic pressure:

$$\frac{\partial U}{\partial t} + U \frac{\partial U}{\partial x} + V \frac{\partial U}{\partial y} + g \frac{\partial \zeta}{\partial x} + F_{sec,x} = -\frac{1}{\rho_0} P_x + \nu_H \left( \frac{\partial^2 U}{\partial x^2} + \frac{\partial^2 U}{\partial y^2} \right) \quad (1)$$

$$\frac{\partial V}{\partial t} + U \frac{\partial V}{\partial x} + V \frac{\partial V}{\partial y} + g \frac{\partial \zeta}{\partial y} + F_{sec,y} = -\frac{1}{\rho_0} P_y + \nu_H \left( \frac{\partial^2 V}{\partial x^2} + \frac{\partial^2 V}{\partial y^2} \right) \quad (2)$$

$$\frac{\partial \zeta}{\partial t} + \frac{\partial [hU]}{\partial x} + \frac{\partial [hV]}{\partial y} = 0 \quad (3)$$

where  $U$  denotes the depth-averaged velocity component in the  $x$  direction ( $\text{m s}^{-1}$ ) and  $V$  the depth-averaged velocity component in the  $y$  direction ( $\text{m s}^{-1}$ ),  $t$  the time (s),  $g$  the acceleration due to gravity ( $\text{m s}^{-2}$ ),  $P$  the hydrostatic pressure ( $\text{N m}^{-2}$ ),  $\zeta$  the water surface elevation (m),  $h$  the water depth (m),  $\nu_H$  the horizontal eddy viscosity ( $\text{m}^2 \text{s}^{-1}$ ),  $\rho_0$  the density of water ( $\text{kg m}^{-3}$ ), and  $F_{sec,x}$  and  $F_{sec,y}$  correction terms to account for the effect of secondary flow on the depth-averaged momentum equations. The detailed description of Delft3D is beyond the scope of this paper and can be found in [10].

The 2D-module accounts for the spiral flow, which is a clear three-dimensional flow feature, by means of a secondary flow model (see [4] for some more details). The time step was 30 seconds to ensure numerical stability as evaluated by the Courant criterion. The flow model was calibrated using the aforementioned discharge of  $615 \text{ m}^3 \text{ s}^{-1}$  for which water surface elevations were available. The values of the calibration parameters and the closure coefficients for the  $k-\epsilon$  model are given in Table 1.

**Table 1.** Calibrated parameter values.

Physical parameter	Calibrated value
Secondary flow correction factor ( $\beta_c$ )	1 (-)
Manning's roughness $n$ value	0.054 ( $\text{s m}^{-1/3}$ )
Horizontal eddy viscosity	1 ( $\text{m}^2 \text{s}^{-1}$ )
Horizontal eddy diffusivity	10 ( $\text{m}^2 \text{s}^{-1}$ )

Following the calibration, the discharge hydrograph for the period 2003-2013 (see Fig. 2) was specified at the upstream boundary and a corresponding time-series of water surface elevations was set as a boundary condition at the downstream boundary. Note that the water levels were based upon a rating curve that was constructed by extending the downstream boundary to Taraghat station (ca. 33.3 km downstream of the study site) and performing hydraulic calculations using the stage-discharge relationship at Taraghat station (137A).

### 3.2. Sediment transport and morphodynamics

For the simulations, a bed porosity of  $\phi = 0.40$  and the sediment size from the study area ( $D_{50} = 0.1$  mm) was used assuming a density of  $2650 \text{ kg m}^{-3}$ . Sediment transport was computed by the total load transport formula of [11]:

$$S_b = \alpha_{EH} \frac{0.05U^5}{\sqrt{gC\Delta^2 D_{50}}} \quad (4)$$

where  $S_b$  is the total sediment transport rate per unit width ( $\text{m}^2 \text{ s}^{-1}$ ),  $\Delta$  is the relative mass density of sediment under water (-),  $D_{50}$  is the median sediment diameter (m), and  $\alpha_{EH}$  is a calibration coefficient ( $O(1)$ ). At the inflow boundary, the sediment transport rate was assumed to be equal to the sediment transport capacity. The bed level was updated after each time step using the Exner equation:

$$\frac{\partial z_b}{\partial t} = MORFAC \left[ \frac{\partial S_{b,x}}{\partial x} + \frac{\partial S_{b,y}}{\partial y} \right] \quad (5)$$

The cross-sectional data from 2013 were exploited to calibrate the morphodynamic model. The calibration coefficient for sediment transport rate ( $\alpha_{EH}$ ) was adjusted to 1.8 to match measured and modelled bed level changes. The calibration factors to account for the spiral flow effect on bed-load transport direction ( $E_s$ ) and transverse bed slope effects ( $\alpha_{bn}$ ) were adjusted to 1.7 and 16, respectively. Since the bank erosion algorithm of Delft3D is based on the distribution of the erosion between the source wet cell and the adjacent dry cell, a factor for erosion of adjacent dry cells was set to 1 so that channel migration and sand movement could be simulated. Finally, to reduce computational time, a morphological scale factor (*MORFAC*) of 10 was used for the bed level changes. More details on the model setup and calibration can be found in [4].

## 4. Results and discussion

### 4.1. Bed topography change

The bed level change is the result of sediment transport, secondary flow effect on bed-load transport direction, bed slope effects, bank erosion, and mass conservation of the bed. Taking these factors into account, the river alignment and bed topography as shown in Fig. 3(a) were obtained from the model for a simulation period of 10 years (2003-2013).

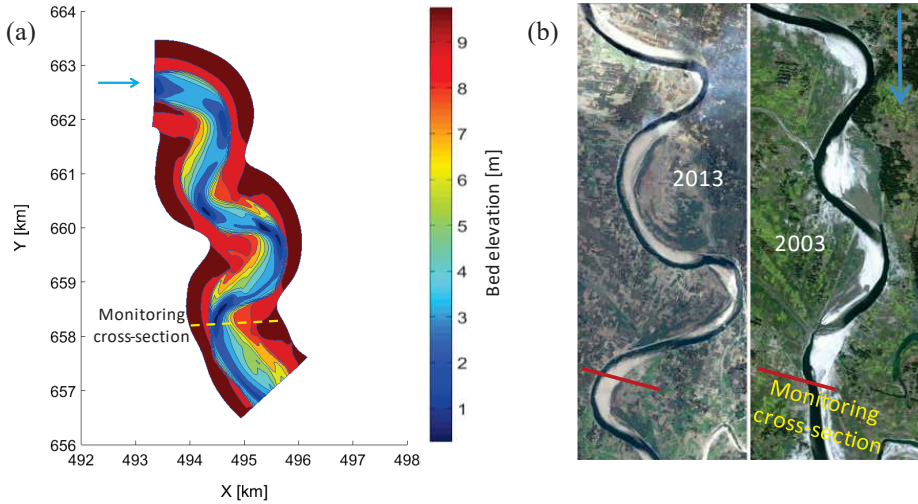


**Fig. 3.** (a) Simulated bed topography and (b) planform images (© Google Earth) of the study area.

The upstream 1 km of the 8.2 km long study reach was not considered for the analysis to avoid effects originating from the upstream boundary conditions. Lateral channel migration led to an increase of the channel bend amplitude and channel length. The increase of bend amplitude resulted in a downstream migration of the meander bends, leading to the development of a more sinuous meandering thalweg. The comparison of the model results (Fig. 3a) with the available field data (Fig. 3b) indicates that the model predicts correctly the locations and patterns of bank migration.

Fig. 4 shows the comparison of the measured and modelled transverse bed profiles. The modelled cross-section is asymmetric in shape with gently sloping inner banks, a deep thalweg near the outer bank, and near vertical outer bank. The observed bank retreat of about 400 m and bank advance of about 210 m are accurately reproduced by the model. However, the transverse bed slope predicted by the model is too shallow in relation to the field data. A deeper analysis of the results revealed that this is associated with the numerical model's limitations in representing the transverse bed slope [4].

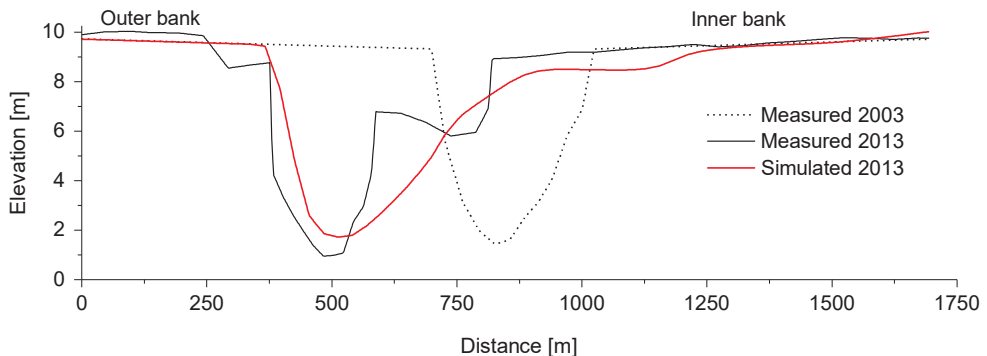


**Fig. 4.** Comparison of observed and simulated bed topography in 2013 at the monitoring cross-section as shown in Fig. 3.

#### 4.2. Planform change

The commonly used parameters to describe the meander planform are meander belt width ( $M_B$ ), meander wavelength ( $\lambda$ ), radius of curvature ( $R$ ) and bankfull width ( $B$ ) (Fig. 5).

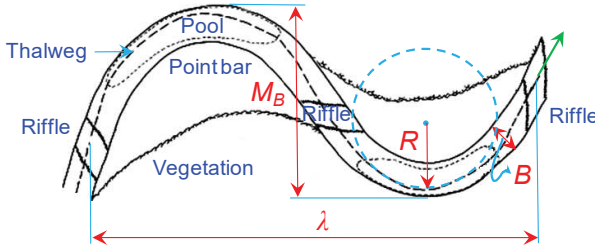


**Fig. 5.** Definition of key planform parameters:  $M_B$  is the meander belt width which is defined as the distance between tangents drawn at the outside of the meanders;  $\lambda$  is the meander wavelength which is defined as the distance between two subsequent inflection points of the wave pattern;  $R$  is the radius of curvature which is defined as the radius of a circular arc that best fits a meander loop and  $B$  is the channel width which denotes bankfull width (modified after [12]).

For the investigation of the planform evolution, the thalweg was extracted from the model results and smoothed by means of cubic spline interpolation using a specifically developed Matlab script. First, curvature values were calculated along the thalweg using an interval length of 1 m. A moving average technique was subsequently applied for smoothing noisy  $x, y$  coordinate data using a 4th-degree polynomial filter (averaging window of three nodes). The smoothed thalweg was split at each inflection point where a change in the direction of curvature occurred. Accordingly, the four meander bends were defined by the location of inflection point. Planform parameters (i.e.,  $M_B, \lambda$  and  $R$ ) were determined according to the definitions shown in Fig. 5. These parameters were normalized by the channel width ( $B$ ) derived from field data rather than by using simulation results as the modelled channel width was poorly predicted in comparison to other parameters. Fig. 6 shows a comparison of the model results with the field observations. In the figure, the dashed lines show the 23% error boundaries for  $M_B/B$ , the 29% error boundaries for  $\lambda/B$ , and the 48% error boundaries for  $R/B$ , respectively.

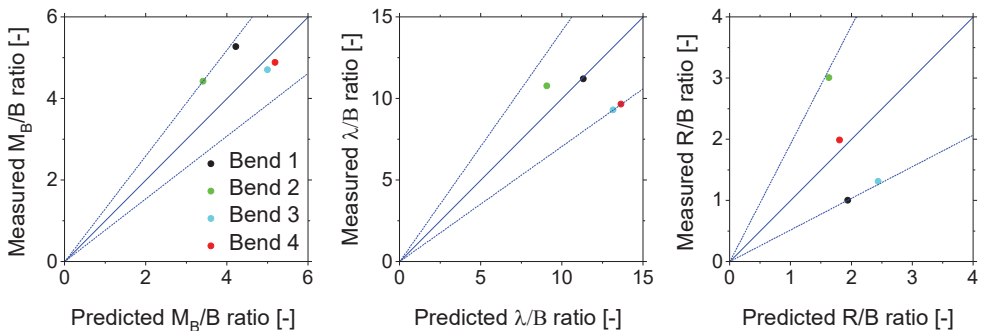


**Fig. 6.** Comparison of model results and observations (a) meander belt width to channel width ratio  $M_B/B$  (the dashed lines show the 23% error boundaries), (b) meander wavelength to channel width ratio  $\lambda/B$  (the dashed lines show the 29% error boundaries) and (c) radius of curvature to channel width ratio  $R/B$  (the dashed lines show the 48% error boundaries).

The computed reach-averaged values of  $M_B/B, \lambda/B$  and  $R/B$  were 4.46, 11.80, and 1.96, respectively. These results are in accordance with results reported in the literature (e.g., [13-14]). Hence it can be concluded that it is possible to capture the dynamics of meandering rivers in terms of both the evolution of bed topography and channel planform using a 2D modelling approach, although it needs to be highlighted that the channel width from field observations has been used for normalization instead of the computed channel width.

## 5. Conclusions

Delft3D can solve three-dimensional flow and associated sediment transport phenomena, but for computational efficiency a depth-averaged 2D model was used in this study. The 2D modelling approach with a parameterization for secondary flow, which is characteristic for curved channels, was used to reproduce bed topography and planform adjustment in the Dhaleshwari River for a period of 10 years (2003-2013). Model parameters were calibrated using measured water level and bed level data. The results showed that the morphological characteristics such as scour depth, bank erosion and locations of pool-riffle morphology were predicted reasonably well, even though the model showed some deficiencies to reproduce bankfull width. Regarding the planimetric evolution, the planform parameters (i.e., meander belt width, meander wavelength and radius of curvature) confirmed that the model results are realistic and that they are in accordance with results reported in the literature (e.g., [13-14]). To date, 2D models have been applied to model meander evolution over periods of days to weeks (e.g., [15]), without providing a basis for assessing the ability of a model to simulate morphological development over decadal time scale. The conclusion from this research is that a 2D modelling approach can capture the natural dynamics of meandering rivers, in terms of both the evolution of bed topography and channel planform.

## References

1. M.S. Banda, S. Egashira, *Sustainable hydraulics in the era of global change*, Proc. 4th IAHR Eur. Congr. (2016)
2. A.C. Schwendel, A.P. Nicholas, R.E. Aalto, S.G.H. Sambrook, S. Buckley, *Earth Surf. Proc. Land.* **40**, 15 (2015)
3. N.R.B. Olsen, *J. Hydraul. Eng.* **129**, 5 (2003)
4. M.S. Banda, *Morphological development of meandering rivers due to discharge reduction*, PhD thesis, TU Braunschweig (to be published)
5. M. Guan, N.G. Wright, P.A. Sleigh, S. Ahilan, R. Lamb, *Water Resour. Res.* **52**, 8 (2016)
6. K. Asahi, Y. Shimizu, J. Nelson, G. Parker, *J. Geophys. Res. Earth Surf.* **118**, 2208-2229 (2013)
7. F. Schuurman, Y. Shimizu, T. Iwasaki, M.G. Kleinmans, *Geomorphology.* **253**, 94-109 (2016)
8. CEGIS, *Report on the Dhaleshwari River under the study on 'Morphological analysis of various rivers in support of RTW Hydro-technical investigation on major rivers'*. Center for Environmental and Geographic Information Services, Dhaka (2013)
9. J.E. Nash, J.V. Sutcliffe, *J. Hydrol.* **10**, 3, 282-290 (1970)
10. G.R. Lesser, J.A. Roelvink, J.A.T.M.V. Kester, G.S. Stelling, *Coast. Eng.* **51**, 883-915 (2004)
11. F. Engelund, E. Hansen, *A monograph on sediment transport in alluvial streams*, Tech. Univ. of Denmark, Technisk Forlag (1967)
12. L.B. Leopold, M.G. Wolman, *Geol. Surv. Prof. Pap.* **282B** (1957)
13. L.B. Leopold, M.G. Wolman, *Geol. Soc. of America Bull.* **71**, 6 (1960)
14. G.P. Williams, *J. Hydrol.* **88**, 147-164 (1986)
15. E. Kasvi, P. Alho, E. Lotsari, Y. Wang, A. Kukko, H. Hyypä, J. Hyypä, *Hydrol. Proc.* **29**, 1604-1629 (2015)